Effect of Airflows on Repetitive Nanosecond Volume Discharges*

TANG Jingfeng (唐井峰)[1], WEI Liqiu (魏立秋)[1], HUO Yuxin (霍玉鑫)[2], SONG Jian (宋健)[2], YU Daren (于达仁)[2], ZHANG Chaohai (张潮海)[3]

[1]Academy of Fundamental and Interdisciplinary Sciences, Harbin Institute of Technology, Harbin 150001, China

[2]School of Energy Science and Engineering, Harbin Institute of Technology, Harbin 150001, China

[3]School of Electrical Engineering and Automation, Harbin Institute of Technology, Harbin 150001, China

Abstract Atmospheric pressure discharges excited by repetitive nanosecond pulses have attracted significant attention for various applications. In this paper, a plate-plate discharge with airflows is excited by a repetitive nanosecond pulse generator. Under different experiment conditions, the applied voltages, discharge currents, and discharge images are recorded. The plasma images presented here indicate that the volume discharge modes vary with airflow speeds, and a diffuse and homogeneous volume discharge occurs at the speed of more than 35 m/s. The role of airflows provides different effects on the 2-stage pulse discharges. The 1st pulse currents nearly maintain consistency for different airflow speeds. However, the 2nd pulse current has a change trend of first decreasing and then rapidly increasing, and the value difference for 2nd pulse currents is about 20 A under different airflows. In addition, the experimental results are discussed according to the electrical parameters and discharge images.

Keywords: volume discharge, airflow, repetitive nanosecond pulse discharge

PACS: *52.25.Fi, 52.30.Ex*

DOI: 10.1088/1009-0630/18/3/10

(Some figures may appear in colour only in the online journal)

1 Introduction

In recent years, repetitively pulsed power technology has undergone a significant development with the improvement of switch and energy-storage technology, and the atmospheric pressure plasmas generated by repetitive nanosecond discharges have received considerable attention for their wide industrial applications such as waste gas (water) treatment, pollution control and synthesis of nanostructure material [1]. Among these plasma applications, a large volume discharge in atmospheric pressure is currently one of the most widely proposed methods. The key to an optimal application performance lies in how to generate stable and diffuse plasma in atmospheric pressure especially in a large volume. Therefore, experimental and theoretical studies of the volume discharge characteristic are required for the various applications of very fast rise time and short-duration electric fields with an order of nanosecond pulses.

In a stationary condition, a volume glow discharge with no filaments has be created in air [2,3], which was not stable and likely to undergo a transition from glow to filamentary or spark mode. The volume discharge was mainly attributed to an appearance of kilovolt energy fast electrons, and the fast electrons provided effective pre-ionization for the resulted formation of a volume discharge [4]. The modes of volume discharge strongly depended on applied pulse rise time and discharge dynamics [5]. Shortening the pulse duration or modifying the electrode geometry was an efficient method to control the mode transition from glow to spark state [3−5].

In order to generate stable and diffuse plasma, airflows have been introduced to atmospheric pressure discharges [6−11], as well as investigating the potential performance of plasma-assisted flow control [12,13]. Luo H Y investigated the effects of gas flows on helium DBD discharges, and provided that the helium flow induced an increase in the density of helium metastables after discharge and thus an enhanced contribution of these metastables to the next breakdown of the helium gap at a lower voltage [6]. Dong L F and Ren C S separately demonstrated airflow effects on the mode DBD discharge with a sinusoidal excitation [7,8]. Pang L studied the effects of low-speed airflow on the surface discharge plasma characteristics by a repetitive nanosecond pulse excitation, and demonstrated a repetitive nanosecond surface discharge in airflow conditions [9]. Pavon S investigated the interaction between high-speed gas flows

*supported by National Natural Science Foundation of China (Nos. 51006027, 51437002, and 51477035)

and surface DBD discharges [10]. Our previous works provide a repetitive nanosecond volume diffuse discharge under airflows, and demonstrate the change of discharge currents imposed by airflows [11].

In order to get a better understanding of the airflow effects on volume discharge characteristics, this paper presents our study of repetitive nanosecond volume discharge behaviors in high-speed airflows. The applied voltage, discharge current, and discharge image are obtained and used to study the effects of airflows on the volume discharges. Then, discharge characteristics are discussed according to the electrical parameters and discharge images.

2 Experimental setup

The experimental system is shown in Fig. 1, which includes a subsonic air wind tunnel, a nanosecond pulse generator, discharge systems, and measurement systems. By changing the air pressure provided for the wind tunnel, the airflow speed at the end of the wind tunnel can be adjusted with a maximum value of up to 250 m/s. A pilot tube is used to measure the airflow speeds. The plate-plate electrodes separated by a 6 mm vertical distance are set in a horizontal and parallel manner. The two electrodes are composed of stainless steel plates with the size of 40 mm×100 mm and a thickness of 2 mm. The electrode edges are fully polished in order to avoid the point discharge occurring at the electrode edges. The two dielectrics are made of mica with a permittivity $\varepsilon_r = 6$ and a thickness of 1 mm. The discharge system is installed at the downstream of the wind tunnel exit, and with the flow direction perpendicular to the electrode surface.

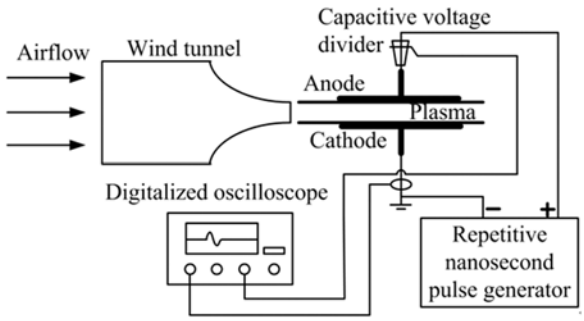

Fig.1 Schematic of experimental setup

Both the applied voltage and the discharge current are the important parameters determining the electrical characteristics. The measurement arrangement is also shown in Fig. 1. Similar to the measurement described in works [3,14], wide bandwidth probes are required to monitor the electrical properties of nanosecond pulse discharges. A capacitive voltage divider is connected to the high-voltage output as the voltage probe, and the voltage ratio of this probe is about 2200. Simultaneously, the total discharge current (including the current across the plate-plate gap to ground) is also measured by a Pearson 6585 Rogowski coil with a response time of less than 1 ns. The voltage signal is relatively stable, and is set as the reference signal to trigger the oscilloscope in experiments. The applied nanosecond voltage pulses have an adjustable amplitude, a fixed pulse width of 10 ns and a fixed rise time of 5 ns, corresponding to the frequency ranging from 10 Hz to 3800 Hz, respectively. The typical luminous images are obtained from the side view, and with the direction perpendicular to the flow speed.

3 Experimental results

3.1 Discharge characteristics under airflows

With an applied pulse voltage of 19 kV, and a pulse repetitive frequency of 1800 Hz (PRF= 1800 Hz), the applied voltage and current waveforms under different airflows are shown in Fig. 2. It is provided that the plate-plate DBD discharge is characterized by a series of 2-stage pulse currents. The discharge current distributes irregularly, which can be attributed to the random nature of breakdown and complicated dynamics in the air gap. It can be drawn that the 1st pulse current is more slightly influenced than that of the 2nd pulse.

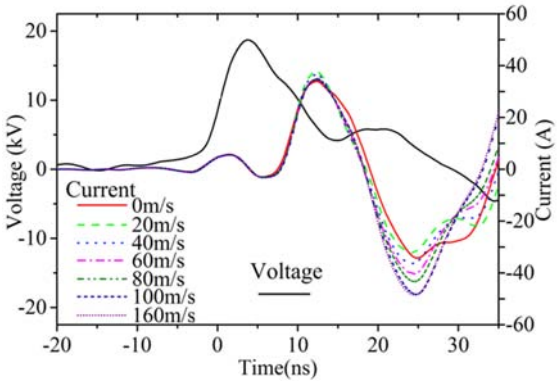

Fig.2 Applied voltage and discharge current waveforms under airflows

There are some discharge modes determined by many factors, and a homogeneous discharge can be obtained with a fast pulsed excitation under some special conditions [15,16]. In order to focus on the airflow influences on the discharge characteristics, several airflow speeds are selected at a given pulsed excitation. The applied voltage has an amplitude of 20 kV, a rise time of 5 ns, a pulse width of 10 ns and a pulse repetitive frequency of 1800 Hz, respectively. The typical luminous discharge images under airflows are obtained, as shown in Fig. 3.

In the quiescent air (i.e., the flow velocity is 0 m/s), a multichannel and inhomogeneous violet discharge is present in the discharge volume. The discharge filaments are straight, and the filament feet are randomly and extensively distributed on the dielectric surface, as shown in Fig. 3(a). Increasing the flow velocity to 10 m/s, the number of the bright filaments is slightly

reduced, but the change of glow component cannot be clearly observed, as shown in Fig. 3(b). When the flow velocity varies from 10 m/s to 20 m/s, the filament number is gradually reduced, and the change of discharge luminance and distribution is relatively little. When the airflow with a speed of 35 m/s is introduced into the volume discharge, as shown in Fig. 3(c), interestingly, a diffuse discharge in a large volume is promoted. The unsteady nature of the filamentary part of the discharge cannot be easily observed with the naked eye in the discharge volume. The diffuse and homogeneous discharge mostly occurs at the middle region, and filament discharge occurs mainly at the inlet region and partly at the exit region of the channel. The filament channels on the two sides may be connected to the electric field concentration occurring at the electrode edges. With the increasing of airflow speeds, the volume discharge modes vary from filament to diffuse modes. Further improving the airflow speed to 50 m/s, as shown in Fig. 3(d), a diffuse discharge also occurs at the middle discharge region, as well as with a reduction of luminous intensity.

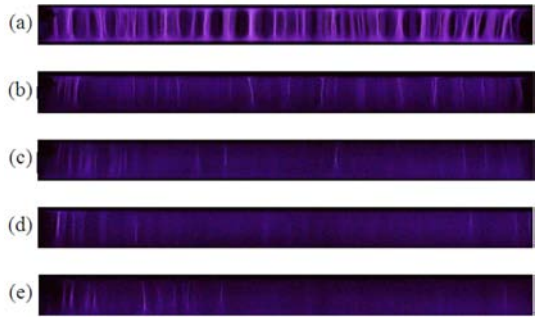

Fig.3 Discharges at different airflow speeds. (a) Flow speed $v = 0$ m/s, (b) $v = 10$ m/s, (c) $v = 35$ m/s, (d) $v = 50$ m/s, and (e) $v = 100$ m/s. Exposure time is 1/1250 s

Moreover, several excitation conditions are selected for the detailed investigation of airflow effects, in which the applied voltage amplitude is chosen from 10 kV to 30 kV, PRF is selected from 100 Hz to 3800 Hz, and airflow speed is changed from 0 m/s to 200 m/s, respectively. In a quiescent air or under a low speed, it presents filament and inhomogeneous violet discharges in a large volume, as likely shown in Fig. 3(a). At such airflow speeds, the number of the bright filaments is slightly increased with only increasing the applied voltage, as a process of the pinch of several filaments. However, the change of discharges cannot be clearly observed with only changing PRFs. With a speed less than 30 m/s, there are less filaments in the volume, and the change of discharge luminance is relatively little with changing the applied voltages and PRFs. With the airflow speed increasing higher, for example a speed of 50 m/s as shown in Fig. 3(d), the relative uniform discharge in a large volume is promoted. Importantly, the discharge becomes unstable and almost fades away at a PRF of less than 220 Hz.

3.2 Effect of airflows on discharge currents

As indicated in Fig. 2, there is a series of 2-stage pulse currents for each one nanosecond pulsed discharge. Even considering the existence of discharge delays, the 1st pulse currents always occur with the same breakdown voltage and at the same breakdown time point. Furthermore, it can be drawn from Fig. 4 that the 1st pulse currents increase first and then reduce with airflow speeds. With the flow speed increasing from 0 m/s to 20 m/s, the amplitude of the current rapidly increases from 33.1 A to 36.3 A at a PRF of 3800 Hz, and then slowly decreases to about 34 A. It goes across a reverse 'V' curve with a turning point at the flow velocity of 20 m/s. The change of 1st pulse current values imposed by airflows is 4 A. Importantly, there are some factors leading to measurement errors in this work, which mainly include the pressure instability of air supplied to the wind channel, the measurement errors of airflow speed with the pilot tube, and the high frequency noises concerned with nanosecond discharges.

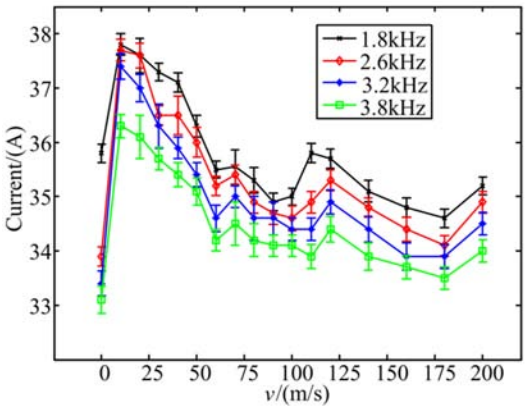

Fig.4 1st pulse currents under airflows at different PRFs

It is clearly shown in Fig. 5 that the 2nd pulse currents are influenced by the addition of airflows to the discharge zone. The 2nd pulse currents almost occur at the same time point. At a PRF of 1800 Hz, the 2nd pulse current has a rapid but small change from −34 A to −32 A with the airflow speed increasing from 0 m/s to 20 m/s, follows with a rapid and big change from −32 A to −47 A, and then becomes gradually relatively stable as the airflow speed is bigger than 80 m/s. It is mostly concerned that the difference between 2nd pulse current values is about 20 A for different airflows.

When the nanosecond pulse discharge is operated at a much lower pulse repetition rate, for example 250 Hz with a 10 m/s airflow, all individual pulse images show a filamentary discharge structure such as the pulse picture shown in Fig. 3(a), which demonstrate random characteristics of filaments formed by nanosecond pulse excitation. Decreasing the PRF to a smaller value, there are no discharges even in the quiescent air condition. Importantly, the discharge became unstable and almost faded away at a PRF of less than 220 Hz.

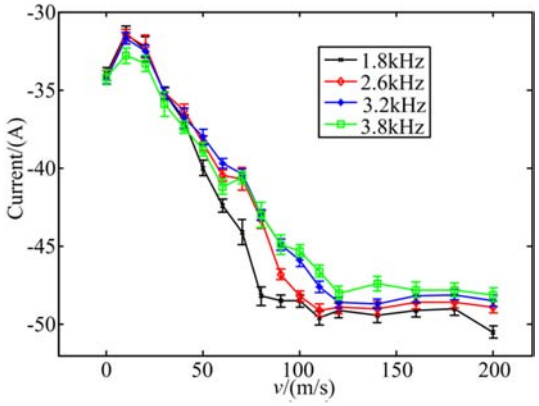

Fig.5 2nd pulse currents under airflows at different PRFS

4 Discussion

As a nanosecond pulse is applied to a plate-plate gap, initial electrons are accelerated by the electric field, and an avalanche process is followed under the electron multiplication of collision ionization. Fast electrons with high energy can run away from the head of the critical avalanche and dominate in the subsequent development of the critical avalanche. When the head of the critical avalanche reaches near to the anode, a discharge bridges is built up between the two dielectrics as well as electrodes, and a discharge current runs through the gap space, which can be represented as the 1st pulse current. As the applied nanosecond pulse is gone, more electrons accumulated in the dielectric surface near the anode, interact with accumulated positive particles near the cathode, and built up a strong electric field imposed on the discharge space. Such space electric field will induce another avalanche process between the two electrodes, and the 2nd pulse currents arise in our experiments.

When the airflow is added into the gap space, the volume discharge modes vary from filament to diffuse modes, and the induced 2-stage pulse currents are also influenced. These behaviors may be attributed to the combined action of two effects. On one hand, the airflows breathe more species into the discharge volume from upstream to downstream, especially the excited meta-stable state, which causes a decrease in the number of initial electrons. On the other hand, the airflows remove accumulated charges on the surface of the dielectric, which is favorable for the development of discharge.

As the 1st pulse current arises, a bigger voltage pulse with a 5 ns rise time, as well as a stronger electric field is being imposed on the electrodes as one discharge driver. Since the pulse action time is too small, airflows in this period can be considered as "frozen" and without any flow mobility. Therefore, the 1st pulse currents nearly maintain consistency for different airflow speeds. However, at the 2nd pulse current arising, accumulated particles near the electrodes induce a space electric field as another discharge driver. Since this driver always acts for several milliseconds, airflow mobility must be considered in this period. As indicated in Fig. 5, the 2nd pulse currents for quiescent air are bigger than that of airflows with speeds of less than 40 m/s. Since airflows breathe more species, especially under excited meta-stable states, out of the discharge volume, the loss of heavy particles under the force of airflows is unfavorable for the development of discharge. Under airflows with a speed of more than 40 m/s, the 2nd pulse currents are always bigger than those of quiescent air; it is concerned with the distribution change of accumulated charges on the surface of the dielectrics by the force of airflows, which is favorable for the development of discharge. With the speed increasing to more than 80 m/s, the 2nd pulse currents become gradually relatively stable, which seem unaffected by airflows. The detail effects under such high airflow speeds are very interested, and also need to be taken into consideration in future works.

5 Conclusion

The effect of airflows on repetitive nanosecond pulse discharges with a plate-plate electrode configuration has been investigated. The results show that the volume discharge in the gap strongly depends on the airflows, and the corresponding images show that the discharge modes vary from filament to diffuse modes with the addition of airflows. A diffuse and homogeneous volume discharge occurs at the airflow speed of more than 35 m/s. Detailed works are carried out to demonstrate the role of the airflows effects on the 2-stage pulse currents by nanosecond pulse discharges. The 1st pulse currents nearly maintain consistency for different airflow speeds. However, the 2nd pulse current has a change trend of first decreasing and then rapidly increasing, and the value difference for 2nd pulse currents is about 20 A under different airflows. The pulse repetitive frequency plays an important role and a pulse repetitive frequency of more than 220 Hz is needed to generate astable discharge under airflow conditions. Further work will be concentrated on the production and control of a volume discharge in airflows, as well as on studying the physical mechanism of various discharge modes.

Acknowledgments

We would like to thank Ren Chunsheng for joint research on repetitive nanosecond volume discharges.

References

1 Lu X P, Yan P, Ren C S, et al. 2011, Scientia Sinica: Phys., Mech. & Astron., 41: 801 (in Chinese)
2 Namihira T, Tsukamoto S, Wang D, et al. 2000, IEEE Transactions on Plasma Science, 28: 434
3 Shao T, Long K, Zhang C, et al. 2008, Journal of Physics D: Applied Physics, 41: 215203

4 Kostyrya I D, Skakun V S, Tarasenko V F, et al. 2004, Tech. Phys., 49: 987
5 Repev A G, Repin P B, Danchenko E G. 2008, Tech. Phys., 53: 858
6 Luo H Y, Liang Z, Wang X X, et al. 2008, Journal of Physics D: Applied Physics, 41: 205205
7 Dong L F, Li S F, Liu F C, et al. 2005, Transactions of Beijing Institute of Technology, 25: 8
8 Wang Z, Ren C S, Nie Q Y, et al. 2009, Plasma Science and Technology, 11: 177
9 Pang L, Zhang Q, Ren B, et al. 2011, IEEE Transactions on Plasma Science, 39: 2922
10 Pavon S, Dorier J, Hollenstein C, et al. 2008, Journal of Physics D: Applied Physics, 40: 1733
11 Tang J F, Wei L Q, Li N, et al. 2014, IEEE Transactions on Plasma Science, 42: 753
12 Li Y H, Wang J, Wang C, et al. 2010, Plasma Sources Science and Technology, 19: 025016
13 Kriegseis J, Grundmann S, Tropea C. 2012, Physics of Plasmas, 19: 073509
14 Shao T, Sun G, Yan P, et al. 2006, Journal of Physics D: Applied Physics, 39: 2192
15 Pai D, Lacoste D A, Laux C O. 2008, IEEE Transactions on Plasma Science, 36: 974
16 Tardiveau P, Moreau N, Bentaleb S. 2009, Journal of Physics D: Applied Physics, 42: 175202

(Manuscript received 9 September 2015)
(Manuscript accepted 1 December 2015)
E-mail address of TANG Jingfeng: tangjingf@hit.edu.cn